Aerosolized α_1 adrenoreceptor antagonism does not affect experimentally induced lung fibrosis in animal models

Short Title: Aerosolized α_1-AR antagonism does not affect lung fibrosis

Alexander Ghincea[1], Carrighan Perry[1], Angela Liu[1], John McGovern[1], Sheeline Yu[1], Xue-Yan Peng[1], Genta Ishikawa[1], Thomas Barnthaler[1], Erica L. Herzog[1,2], Huanxing Sun[1*]

[1]Section of Pulmonary, Critical Care, and Sleep Medicine, Department of Internal Medicine, Yale University School of Medicine, New Haven, Connecticut, United States of America
[2]Department of Molecular Medicine and Experimental Pathology, Yale University School of Medicine, New Haven, Connecticut, United States of America

*Corresponding author
Email: huanxing.sun@yale.edu (HXS)

Abstract

Pulmonary Fibrosis is a progressive and incurable condition that complicates many disease states. Adrenergic hyperinnervation and accumulation of fibroblasts expressing α_1-adrenoreceptors have been implicated in this process. Previous studies have demonstrated that systemic treatment with an α_1-adrenoreceptors antagonist attenuates fibrotic endpoints in lung fibrosis models. In an attempt to develop a lung targeted therapy, we determined whether α_1-adrenoreceptors antagonism delivered via inhaled administration of terazosin exerts antifibrotic benefits in experimentally induced lung fibrosis. C57/BL6 mice treated with bleomycin, or a doxycycline inducible line of transgenic mice with lung specific overexpression of the bioactive form of the human TGFβ1 (*TGFβ1-Tg*$^+$ model), received nebulized terazosin at varying doses on a therapeutic schedule following the induction of fibrosis and were sacrificed at 21 days. Airway inflammation, fibrotic endpoints, and lung function were evaluated. α_1-adrenoreceptors antagonism delivered via this method did not impact airway inflammation as indicated by bronchoalveolar lavage cell counts, and there was no significant difference observed in soluble collagen content. There was similarly no significant difference in respiratory mechanics with terazosin administration. These data show that inhaled delivery of the α_1-adrenoreceptors antagonist terazosin by this method is ineffective at treating fibrosis in these models and suggest that alternative dosing schedules or delivery methods may be more fruitful avenues of investigation. Further exploration of these findings may provide new therapeutic options and illuminate mechanisms through which adrenergic innervation and α_1-adrenoreceptors mediate fibrosis in the adult mammalian lung.

Introduction

Pulmonary fibrosis (PF) is an incurable condition that complicates numerous interstitial lung diseases and is characterized by progressive pulmonary fibrosis and lung function decline [1, 2]. The incidence and demographic distribution of PF is heterogenous depending on underlying diagnosis but tends to occur in older adults and is often associated with a poor prognosis [3]. Idiopathic pulmonary fibrosis (IPF), one of the better studied forms of PF, is defined by a pattern of usual interstitial pneumonia on imaging and histopathology in the absence of a known cause and has a median survival of 2-4 years [4, 5]. Though the underlying pathologic mechanisms vary, pulmonary fibrosis is thought to be the result of dysregulated lung healing that results in the accumulation of activated fibroblasts and excessive extracellular matrix [6-8]. Despite numerous recent advances, treatments remain limited and lung transplantation is the only cure [4, 9]. Thus, considering the significant morbidity and mortality caused by these diseases, there is an urgent need for new targeted interventions to reduce the burden of fibrosis.

Noradrenergic mechanisms are increasingly associated with numerous pathologic processes including acute inflammation [10, 11], innate immune activation [12, 13], cancer [14], obesity and metabolism [15], bone marrow aging [16], and pathologic lung remodeling [17-19]. Adrenergic hyperinnervation and the accumulation of α_1-adrenoreceptor (α_1-AR) expressing cells are associated with fibrosis in animal models, where interruption of adrenergic signaling via chemical denervation and α_1-AR antagonism mitigates fibrotic endpoints [17, 19]. It has further been shown that in some settings the blood [20] and lungs [19] of IPF patients are enriched for noradrenaline, and that IPF patients prescribed α_1-AR antagonists for non-pulmonary indications experience improved survival [19]. However, despite the increasing association of noradrenaline and fibrotic lung remodeling, the mechanisms of this effect and its therapeutic potential remain unexplored [21, 22].

99 Pulmonary expression of α_1-ARs is the best characterized in smooth muscle cells of the
100 airways and vasculature, where they are reported to mediate noradrenaline-induced contractile
101 responses [23, 24]. Interestingly, this receptor class is also expressed in parenchymal
102 endothelium and fibroblasts [25], which may, in part, account for the capillary leak-associated
103 fibroblast activation and extracellular matrix expansion caused by intravenous infusion of the α_1-
104 AR agonist phenylephrine [26, 27] and the therapeutic benefit of systemically administered α_1-
105 AR antagonism delivered via the oral or intraperitoneal routes [17-19]. However, α_1-ARs are
106 also expressed by populations of lung epithelia and airway inflammatory cells which may
107 contribute to noradrenaline's well described role in remodeling responses of apoptosis [28],
108 inflammatory cell trafficking [29], and cytokine production [30]. This expression pattern suggests
109 that interventions leveraging inhaled administration might exert therapeutic benefit while
110 minimizing off-target effects. Elucidation of this biology has the potential to provide insights into
111 the cell(s) and mechanism(s) through which noradrenaline exerts its fibrogenic effects while
112 exploring new treatment modalities [31-33] for parenchymal disease.
113 This study sought to address this knowledge gap by assessing whether inhaled
114 administration of the non-selective α1-AR antagonist terazosin reduces lung inflammation,
115 pulmonary function, biochemical collagen accumulation, and lung histology in two well accepted
116 animal models of experimentally induced fibrosis.
117

118 # Materials and Methods

119 ## Study Design

120 The objective of our study was to test the prespecified hypothesis that nebulized delivery
121 of an α_1-AR antagonist, specifically terazosin, would improve experimentally induced pulmonary
122 fibrosis in two commonly used mouse models. Primary endpoints were prospectively determined.

123 # Animals

124 All animal experiments were approved by the Yale School of Medicine IACUC in
125 accordance with federal regulations (protocol #20292). Twenty-one days following the
126 experimental induction of fibrosis, animals were anesthetized for pulmonary function testing, then
127 humanely sacrificed to isolate bronchoalveolar lavage (BAL), and *en bloc* resection of lungs for
128 soluble collagen quantification and histopathology scoring as we have previously described [34].
129 C57 Black 6 (C57BL/6) wild-type mice were used for bleomycin experiments. TGFβ1 lung specific
130 over-expressing (*CC10-tTS-rtTA-TGFβ1,* from here on called "*TGFβ1-Tg*$^{+}$") mice have been
131 described previously [35] and develop fibrosis in response to doxycycline inducible expression of
132 the bioactive form of the human *TGFβ1* gene under the lung specific CC10 promoter. All
133 experimental groups were matched for age and sex.

134 ## Bleomycin model

135 Sex-matched C57BL/6 aged 9 to 11 weeks mice were exposed to a single dose of 1.5
136 U/kg pharmacologic grade bleomycin (Northstar Rx LLC, NDC 16714-886-0) or sterile saline by
137 orotracheal aspiration [36]. Mice were anesthetized with isoflurane and suspended by their
138 incisors on a standing rack. With the tongue held in gentle retraction, 50 µL bleomycin or saline
139 was pipetted into the oropharynx and aspirated. Animals were sacrificed after 21 days and
140 evaluated for the endpoints described above.

141 ## *TGFβ1-Tg*$^{+}$ model

142 Sex-matched 9 to 11-week-old wild-type *TGFβ1-Tg*$^{+}$ mice received 0.5 mg/mL doxycycline
143 hyclate (Thermo Scientific Cat No. J60579.22) in their drinking water for 21 days as previously
144 described [35].

145 # Nebulization Experiments

146 Starting at day 5 after bleomycin administration or doxycycline initiation, mice received
147 daily administration of nebulized terazosin (Millipore Sigma, Product No. 1643452) dissolved in
148 sterile water at concentrations of 0.001 mg/mL, 0.002 mg/mL, 0.01 mg/mL, 0.02 mg/mL, 0.1
149 mg/mL, and 0.2 mg/mL which were derived to approximate a total inhaled dose of 0.001 mg/kg,
150 0.002 mg/kg, 0.01 mg/kg, 0.02 mg/kg, 0.1 mg/kg, and 0.2 mg/kg per day (Fig S1) [37].
151 Concentrations that showed potential benefit were selected for confirmatory studies. Groups of
152 up to 5 mice from a single cage were placed in a clean plastic box with an attachment for nebulizer
153 tubing in a manner similar to that used by Schroeder et al [38] for drug administration. Omron
154 CompAir NE-C28 compressor nebulizers were used to aerosolize and deliver 7 mL of terazosin
155 or sterile water control on a daily therapeutic schedule over 30 min after which mice were returned
156 to their original cages. The same terazosin dose was repeated for every treatment within each
157 group. A schematic of the nebulizer apparatus is shown in Fig 1A.
158
159 **Fig 1**: **Inhalational administration of the nonselective α_1-AR antagonist terazosin does not**
160 **impact lung inflammation.** ***A***: Experimental design. Inhaled terazosin was started five days after
161 bleomycin administration or doxycycline induced TGFβ1 transgene activation. Up to 5 mice from
162 a single cage were placed into a clean, lidded plastic box with an attachment for nebulizer tubing.
163 7 mL of sterile water or terazosin was loaded into the nebulizer module for each treatment. Tubing
164 connections were checked to be airtight prior to every treatment. Omron NE-C28 compressor
165 nebulizers were used to aerosolize and deliver the treatment over 30 minutes. After treatment
166 mice were returned to their original cages, and the plastic box and nebulizer equipment cleaned
167 thoroughly. ***B***: In the bleomycin model, relative to vehicle, inhaled terazosin had no significant
168 impact on lung inflammation as measured by BAL cell counts. ***C***: In the TGFβ1-Tg$^+$ model, relative
169 to vehicle, inhaled terazosin had no significant impact on lung inflammation as measured by BAL
170 cell counts. Schematic diagrams created using BioRender.com
171

172 ## BAL cell count

173 At the time of sacrifice, two aliquots of 0.8 mL of PBS were slowly instilled into lung and
174 the lavage fluid gently aspirated. The combined BAL sample was assessed for white blood cell
175 counts using a Beckman Coulter Ac.T Diff instrument.

176 ## Pulmonary function testing

177 Pulmonary mechanics and airway hyperresponsiveness were assessed in a subset of
178 terazosin-exposed and control mice from both bleomycin and *TGFβ-Tg*$^{+}$ arms of our study using
179 the Sireq FlexiVent Fx computer-controlled piston ventilator running Flexiware version 7.6 [39].
180 Animals were anesthetized with an intraperitoneally administered mixture of xylazine and
181 ketamine, xylazine (Akorn, NDC 59399-110-20) at a dose of 10 mg/kg and ketamine (Covetrus,
182 NDC 11695-0703-1) at a dose of 100 mg/kg, followed by urethane at a dose between 0.009 to
183 0.03 g per mouse, administered intraperitoneally. Once an appropriate level of sedation was
184 established, a midline neck incision was made, and the soft tissue dissected to expose the
185 trachea. A rigid 20-guage blunt tipped catheter for female mice or 18-gauge blunt tipped catheter
186 for male mice was used to cannulate the trachea. Mice were then paralyzed with pancuronium
187 bromide (Sigma, Cat# P1918-10mg) at a dose of 10 µg per mouse and attached to the FlexiVent
188 for pulmonary function measurements. Methacholine (SigmaAldrich A2251-25G) was used for
189 airway hyperresponsiveness measurements. After completion of lung function testing, mice were
190 humanely euthanized and harvested for tissue as described above.

191 ## Collagen quantification

192 Right lung soluble collagen content was assessed using the Sircol Soluble Collagen Assay
193 (Biocolor Ltd., CLS 1111) according to the manufacturer's instructions.

194 ## Histologic analysis

195 Formalin fixed and paraffin embedded (FFPE) tissue sections obtained from whole left
196 lungs harvested from experimental animals were stained with Masson's trichrome stain to
197 visualize collagen deposition. Modified Ashcroft Scores, a semiquantitative scoring system
198 validated for experimentally induced fibrosis in rodents, were also determined [40].

199 Statistics

200 GraphPad Prism version 9.4.1 was used for statistical analysis and data graphing.
201 Unpaired 2-tailed Mann-Whitney and Kruskal-Wallis tests were used for nonparametric
202 comparisons, and 2-tailed Students T-test and Analysis of Variance used for parametric
203 comparisons. The slopes of expiratory flow-volume loops and airway resistance curves were
204 compared using simple linear regression.
205

206 Results

207 Inhalational administration of an α_1-AR antagonist does not 208 impact lung inflammation

209 α_1-AR antagonists administered via oral or intraperitoneal routes demonstrate antifibrotic
210 benefit in models of cross organ fibrosis including the lung, liver, heart, and kidney [41-44]. To
211 determine whether similar benefit is achieved by local delivery to the lung, the following
212 experiments were performed. Because the benefits of α_1-AR antagonism include attenuation of
213 inflammation [45, 46] and TGFβ1-dependent tissue responses [47], two experimental models
214 were used: single dose inhaled bleomycin, and lung specific, doxycycline inducible
215 overexpression of the bioactive form of the human *TGFβ1* gene. In both models, mice received
216 nebulized terazosin according to a therapeutic schedule (Fig 1A). Doses were determined based
217 on previous literature indicating a 1:1 conversion between systemic and inhaled delivery of the
218 related α_1-AR antagonist, Prazosin [48]. Because α_1-AR antagonism mitigates lung inflammation

219 in a number of contexts, we began by determining whether this treatment might reduce the airway
220 inflammation associated with pulmonary fibrosis in the hyperinflammatory bleomycin mode. The
221 assessment of BAL cell counts in the bleomycin model revealed no significant change following
222 administration of nebulized terazosin at any dose (Fig 1B). Similar findings were seen in the
223 *TGFβ1-Tg*$^+$ model, where BAL cell counts remained essentially unaltered by terazosin (Fig 1C).
224 These data indicate that at the range of doses tested, aerosolized delivery of an α_1-AR antagonist
225 does not impact the magnitude of lung inflammation.
226

227 Inhalational administration of an α_1-AR antagonist does not 228 impact lung compliance or airway resistance

229 Physiologic changes caused by pulmonary fibrosis include the development of restrictive
230 lung physiology and our previous work has shown that patients prescribed α_1-AR antagonists for
231 prostate-related indications exhibited preserved lung compliance as reflected by the forced vital
232 capacity (FVC) [19] and could improve lung compliance without a concomitant increase in airway
233 resistance that could be theoretically induced by α_1-AR signaling [48]. To test this hypothesis,
234 bleomycin-challenged mice that had or had not received inhaled terazosin underwent pulmonary
235 function testing using the FlexiVent system. In the bleomycin model, mean baseline static lung
236 compliance of 0.046 mL/cmH2O (Fig 2A), pressure-volume loops (Fig 2B), and mean baseline
237 maximal airway resistance of 2.96 cmH2O.s/mL assessed following methacholine challenge (Fig
238 2C) were not significantly changed by terazosin administration. Similar findings were observed in
239 the *TGFβ1-Tg*$^+$ mice, where baseline static compliance of 0.044 mL/cmH2O and airway
240 resistance of 5.66 cmH2O.s/mL did not display changes in response to nebulized terazosin (Fig
241 2D-F). These data show that aerosolized delivery of the α_1-AR antagonist terazosin is ineffective
242 in altering lung physiology in two models of fibrotic ILD.
243

244 **Fig 2**: **Inhalational administration of an α_1-AR antagonist does not impact lung compliance**
245 **or airway resistance.** ***A***: Bleomycin-challenged mice that had or had not received inhaled
246 terazosin underwent pulmonary function testing using the FlexiVent system. Here, a mean
247 baseline static lung compliance of 0.046 mL/cmH2O was observed in untreated mice and was
248 not significantly altered by terazosin administration. ***B***: Terazosin did not significantly change the
249 pressure-volume relationship for lungs tested. ***C***: Maximal airway resistance assessed following
250 methacholine challenge did not significantly change following terazosin administration from a
251 mean baseline of 2.96 cmH2O.s/mL in untreated mice. ***D-F***: Similar findings were observed in the
252 TGFβ1-Tg$^+$ mice, where baseline static compliance of 0.044 mL/cmH2O and airway resistance of
253 5.66 cmH2O.s/mL did not display changes in response to nebulized terazosin. These data show
254 that aerosolized delivery of the α_1-AR antagonist terazosin is ineffective in altering lung physiology
255 in two models of fibrotic ILD.
256

257 Inhalational administration of an α_1-AR antagonist does not
258 impact lung collagen accumulation

259 Systemic administration of α_1-AR antagonists has been shown to suppress fibroblast
260 activation and its associated accumulation of collagen in numerous models of organ fibrosis. Our
261 own work and that of others shows that this effect extends to the lungs [17, 19]. Reasoning that
262 local delivery of the α_1-AR antagonist terazosin might show similar efficacy, the lungs of
263 bleomycin-challenged mice that did and did not receive terazosin underwent biochemical
264 quantification of collagen using the well described Sircol assay. Using this approach, fold change
265 from a baseline collagen content per whole right lung was essentially unchanged across all
266 terazosin doses tested (Fig 3A). In the *TGFβ1-Tg*$^+$ model, promising reductions in the fold change
267 from baseline collagen content per whole right lung were observed at several tested terazosin
268 doses (Fig 3B). Based on these results we selected the terazosin doses of 0.002 and 0.02 mg/mL

269 for confirmatory studies but were unable to replicate our initial results (Fig 3C-D). Given these
270 conflicting findings, we sought to confirm our results using histological measures such as
271 trichrome staining and semi-quantitative modified Ashcroft scores, which complement
272 biochemical measures by assessing collagen accumulation in parenchymal regions. The results
273 of these studies were consistent with our confirmatory biochemical measurements, as in the
274 *TGFβ1-Tg*$^+$ model trichrome staining and baseline modified Ashcroft scores was similar at the
275 doses of terazosin assessed (Fig 3E-F). When viewed in combination, our data show that
276 localized delivery of aerosolized terazosin exerts no observable benefit in these models and is
277 insufficient to mitigate lung fibrosis.
278
279 **Fig 3**: **Inhalational administration of an α_1-AR antagonist does not impact lung collagen**
280 **accumulation.** ***A***: Fold change from baseline collagen content per whole right lung was
281 essentially unchanged across all doses tested in bleomycin challenged mice. ***B***: In the TGFβ1-
282 Tg$^+$ model, initial studies revealed a significant difference in fold change from baseline right lung
283 collagen content at 0.002 mg/mL, 0.01 mg/mL, 0.02 mg/mL, and 0.1 mg/mL Terazosin. ***C-D***: Due
284 to these initially promising results confirmatory studies were performed for 0.002 mg/mL and 0.02
285 mg/mL. We were unable to replicate the initially promising differences seen in TGFβ-Tg$^+$ animals
286 at Terazosin doses of 0.002 mg/mL and 0.02 mg/mL. ***E-F***: Trichrome staining and semi-
287 quantitative Modified Ashcroft Scores done in our confirmatory studies did not significantly change
288 after administration of terazosin. These data show that in contrast to the previously reported
289 antifibrotic benefit of systemic α_1-AR, nebulized delivery of this agent is insufficient to mitigate
290 collagen deposition in lung tissues.
291
292
293

294 # Discussion

295 This study aimed to determine whether local delivery of the α_1-AR antagonist terazosin
296 improves markers of pulmonary fibrosis in two different animal models. Our data indicate that the
297 administration of terazosin in nebulized form did not impact lung inflammation, airway compliance
298 or resistance, collagen accumulation, or histologic measures of lung remodeling in the bleomycin
299 and *TGFβ1-Tg*$^+$ models of murine pulmonary fibrosis. These results are in contrast to prior work
300 in which intraperitoneal administration of terazosin modulates fibrotic changes in bleomycin
301 challenged mice [17] and numerous studies demonstrating that α_1-AR blockade improves fibrotic
302 endpoints in cross-organ models of tissue fibrosis including the lung, liver, heart, and kidney [41-
303 44]. Notably, because the present study assessed localized tissue delivery as opposed to
304 systemic α_1-AR antagonism, our data indicate that alternate approaches will be required to
305 support the repositioning of this drug for the treatment of lung fibrosis.

306 The α_1-ARs are a conserved family of G-protein coupled receptors found in numerous
307 tissues including the lung and have been identified both intracellularly and on the extracellular
308 membrane of smooth muscle cells in the airway and pulmonary vasculature, immune cells, and
309 fibroblasts [23, 24, 49]. Additionally α_1-AR agonism has been linked to increased expression of
310 inflammatory markers such as IL-1α, IL-1β, IL-6, and TNF-α both systemically and in the lungs,
311 and prior work has associated this to increased levels of TGFβ [27]. In contrast, systemically
312 delivered α_1-AR antagonism has been shown to attenuate lung inflammation [45, 46] and TGFβ1-
313 dependent tissue responses [47], is associated with improved fibrotic endpoints [41-44] and
314 survival in IPF patients [19]. One interpretation of our conflicting results is that administration of
315 α_1-AR antagonist by nebulized aerosol might only interact with cells locally in the airway and
316 alveolus and may not achieve sufficient uptake to the fibrotic interstitium to exert its effects on the
317 fibroblasts, myofibroblasts, and pericytes that are the primary effectors of fibrosis (Fig 4).
318

319 **Fig 4: Proposed schematics.** ***A***. Schematic of the proposed basic mechanism of terazosin. By
320 non-selectively antagonizing α_1-ARs, Terazosin is proposed to block the pro-fibrotic effects of
321 noradrenaline in the lung. ***B***. Adrenergic nerve density is increased in the fibrotic lung and
322 increased noradrenaline is believed to promote a fibrotic phenotype. Numerous cell types
323 including fibroblasts, myofibroblasts, macrophages, airway epithelial cells, and sympathetic
324 neurons express α_1-ARs, and these are up-regulated in fibrosis. There are several mechanisms
325 which may explain the lack of anti-fibrotic effect observed in our study. When terazosin is
326 nebulized and inhaled, particulate size, dosage, and the heterogeneous nature of fibrotic lung
327 may limit the amount of drug that reaches the terminal airways and alveoli (indicated by more
328 lightly shaded particulates in the schematic). Additionally, though remodeling responses
329 secondary to noradrenaline have been described in the epithelium, the terazosin dose when
330 administered in nebulized form may be insufficient to alter pro-fibrotic signaling. Alveolar
331 macrophages, which are more likely to be exposed to terazosin, may not play as large a role in
332 the development of fibrosis in our model. Finally, transport of terazosin across the basement
333 membrane may also be limited so that insufficient quantities of the drug reach interstitial
334 fibroblasts, myofibroblasts, and pericytes. In contrast, systemic administration of terazosin is more
335 likely to achieve therapeutic levels for α_1-AR antagonism in fibrotic foci. Created with
336 BioRender.com
337
338 Terazosin is a specific α_1-AR antagonist [50] that has been approved for use for decades
339 in the treatment of benign prostatic hyperplasia and hypertension, and has a well-established
340 safety profile [51, 52]. Its long half-life makes it well suited for once daily administration [53].
341 Though there are no prior studies assessing inhalational forms of terazosin, other α_1-AR
342 antagonists have been studied in the context of asthma [54] including a nebulized form of another
343 long acting α_1-AR antagonist Prazosin [48, 55, 56]. While these early studies had limited efficacy

344 in the overall management of asthma, they did indicate that nebulized delivery of α_1-AR
345 antagonists is a viable modality. However, the fibrotic lung is spatially heterogenous with areas of
346 normal tissue interspersed with diseased lung that has mismatched ventilation and perfusion [57].
347 Numerous agents are in development or have been investigated for topical delivery in IPF and
348 recent work has demonstrated that particulate dimension is critically important for adequate drug
349 delivery to fibrotic sites [58]. Specifically, Usmani and colleagues demonstrated that a particulate
350 size of 1.5 μm compared to 6 μm was best for uptake in the fibrotic lung [58]. The Omron CompAir
351 NE-C28 compressor nebulizers used in the present study produce an aerosol particle size of 3
352 μm median mass aerodynamic diameter. While suboptimal based upon the aforementioned
353 study, we believe that this particle size should reach the terminal airways. However, particulate
354 size may yet represent a potential source for the negative results observed in our study. If too
355 large, the particulates may become trapped in the oropharynx, trachea, or larger airways and fail
356 to reach fibrotic regions.

357 Our study is limited in not having assessed the spatial delivery of drug within the mouse
358 lung nor systemic uptake of terazosin into the bloodstream. Target engagement was also not
359 evaluated. Furthermore, our apparatus delivered the aerosolized terazosin into a box containing
360 several mice such that at least some amount of the aerosol was deposited onto the fur of treated
361 animals as well as the interior surface of the container, limiting the quantity of terazosin inhaled
362 into the lungs. Oral ingestion of drug accumulated on the fur or interior surface may further
363 confound our results. Finally, the dose of terazosin administered, or dosing schedule utilized may
364 have been insufficient to achieve adequate penetration or α_1-AR blockade. Recent work by Bai et
365 al using a nanoparticle delivery system presents an alternative method for blocking α_1-ARs that
366 can be investigated in future studies [59].

367

368

369 # Conclusion

370 Aerosolized delivery of the α_1-AR antagonist terazosin is ineffective at treating fibrosis in
371 the bleomycin and *TGFβ1-Tg*$^+$ models of murine pulmonary fibrosis. Given existing data showing
372 benefit from systemic α_1-AR antagonism in fibrotic models, alternative dosing schedules or modes
373 of delivery may be more fruitful avenues of research. Further exploration of these findings may
374 provide new therapeutic options and illuminate the mechanisms through which adrenergic
375 innervation and α_1-ARs mediate fibrosis in the adult mammalian lung.
376

377 # Acknowledgements

378 We are grateful for Dr. Qing Liu's instruction of the operation of the FlexiVent System and the
379 Omron CompAir NE-C28 compressor nebulizer.
380
381
382
383
384
385
386
387
388
389
390
391
392

Supporting information

Fig S1: **Method used to derive Terazosin doses administered.** ***A***: The time (T_f) to fill the box in which mice were placed for nebulization experiments with nebulized drug is represented by the quotient of Box Volume divided by the Nebulizer Flow Rate. Our enclosures have a volume of 6682 mL, and the Omron CompAir NE-C28 nebulizer has a flow rate of 4000 mL/min. ***B***: The aggregate rate (R) at which nebulized drug enters the box is equal to the total Volume of Drug used divided by the Nebulization Time multiplied by the Drug Concentration loaded into the nebulizer. 7 mL of drug was used in our experiments, and based on our observations, the Omron CompAir NE-C28 nebulizer requires approximately 30 minutes to nebulize all 7 mL. ***C***: The drug weight (D_w) of nebulized terazosin within our enclosure is equal to the product of T_f and R. ***D***: When divided by the box volume, this results in the nebulized drug's concentration (D_c) within the box. Minute Ventilation (V_E) is equal to the product of Respiratory Rate and Tidal Volume. The respiratory rate for adult mice is 187 breaths per minute, and the tidal volume 0.061 mL and 0.094 mL for 20g and 25g mice respectively (38). ***E***: Thus, we derive the total dose of drug in milligrams inhaled (D_t) by a single mouse during each 30-minute nebulization treatment to be equal to the product of D_c, V_E, and nebulization time.

418 # References

419 1. Wells AU, Brown KK, Flaherty KR, Kolb M, Thannickal VJ, Group IPFCW. What's in a
420 name? That which we call IPF, by any other name would act the same. Eur Respir J. 2018;51(5).
421 Epub 20180517. doi: 10.1183/13993003.00692-2018. PubMed PMID: 29773608.
422 2. Cottin V, Hirani NA, Hotchkin DL, Nambiar AM, Ogura T, Otaola M, et al. Presentation,
423 diagnosis and clinical course of the spectrum of progressive-fibrosing interstitial lung diseases.
424 Eur Respir Rev. 2018;27(150). Epub 20181221. doi: 10.1183/16000617.0076-2018. PubMed
425 PMID: 30578335; PubMed Central PMCID: PMCPMC9489068.
426 3. Olson AL, Gifford AH, Inase N, Fernandez Perez ER, Suda T. The epidemiology of
427 idiopathic pulmonary fibrosis and interstitial lung diseases at risk of a progressive-fibrosing
428 phenotype. Eur Respir Rev. 2018;27(150). Epub 20181221. doi: 10.1183/16000617.0077-2018.
429 PubMed PMID: 30578336.
430 4. Raghu G, Remy-Jardin M, Richeldi L, Thomson CC, Inoue Y, Johkoh T, et al. Idiopathic
431 Pulmonary Fibrosis (an Update) and Progressive Pulmonary Fibrosis in Adults: An Official
432 ATS/ERS/JRS/ALAT Clinical Practice Guideline. Am J Respir Crit Care Med. 2022;205(9):e18-e47.
433 doi: 10.1164/rccm.202202-0399ST. PubMed PMID: 35486072.
434 5. Raghu G, Chen SY, Yeh WS, Maroni B, Li Q, Lee YC, et al. Idiopathic pulmonary fibrosis in
435 US Medicare beneficiaries aged 65 years and older: incidence, prevalence, and survival, 2001-
436 11. Lancet Respir Med. 2014;2(7):566-72. Epub 20140527. doi: 10.1016/S2213-2600(14)70101-
437 8. PubMed PMID: 24875841.
438 6. Mei Q, Liu Z, Zuo H, Yang Z, Qu J. Idiopathic Pulmonary Fibrosis: An Update on
439 Pathogenesis. Front Pharmacol. 2021;12:797292. Epub 20220119. doi:
440 10.3389/fphar.2021.797292. PubMed PMID: 35126134; PubMed Central PMCID:
441 PMCPMC8807692.
442 7. Ishikawa G, Liu A, Herzog EL. Evolving Perspectives on Innate Immune Mechanisms of
443 IPF. Front Mol Biosci. 2021;8:676569. Epub 20210809. doi: 10.3389/fmolb.2021.676569.
444 PubMed PMID: 34434962; PubMed Central PMCID: PMCPMC8381017.
445 8. Wijsenbeek M, Cottin V. Spectrum of Fibrotic Lung Diseases. N Engl J Med.
446 2020;383(10):958-68. doi: 10.1056/NEJMra2005230. PubMed PMID: 32877584.
447 9. Flaherty KR, Wells AU, Cottin V, Devaraj A, Walsh SLF, Inoue Y, et al. Nintedanib in
448 Progressive Fibrosing Interstitial Lung Diseases. N Engl J Med. 2019;381(18):1718-27. Epub
449 20190929. doi: 10.1056/NEJMoa1908681. PubMed PMID: 31566307.
450 10. Mirakaj V, Dalli J, Granja T, Rosenberger P, Serhan CN. Vagus nerve controls resolution
451 and pro-resolving mediators of inflammation. J Exp Med. 2014;211(6):1037-48. Epub 20140526.
452 doi: 10.1084/jem.20132103. PubMed PMID: 24863066; PubMed Central PMCID:
453 PMCPMC4042652.
454 11. Borovikova LV, Ivanova S, Zhang M, Yang H, Botchkina GI, Watkins LR, et al. Vagus nerve
455 stimulation attenuates the systemic inflammatory response to endotoxin. Nature.
456 2000;405(6785):458-62. doi: 10.1038/35013070. PubMed PMID: 10839541.
457 12. Willemze RA, Welting O, van Hamersveld P, Verseijden C, Nijhuis LE, Hilbers FW, et al.
458 Loss of intestinal sympathetic innervation elicits an innate immune driven colitis. Mol Med.

459 2019;25(1):1. Epub 20190107. doi: 10.1186/s10020-018-0068-8. PubMed PMID: 30616543;
460 PubMed Central PMCID: PMCPMC6322236.
461 13. Grebe KM, Takeda K, Hickman HD, Bailey AL, Embry AC, Bennink JR, et al. Cutting edge:
462 Sympathetic nervous system increases proinflammatory cytokines and exacerbates influenza A
463 virus pathogenesis. J Immunol. 2010;184(2):540-4. Epub 20091216. doi:
464 10.4049/jimmunol.0903395. PubMed PMID: 20018617; PubMed Central PMCID:
465 PMCPMC2941093.
466 14. Zahalka AH, Arnal-Estape A, Maryanovich M, Nakahara F, Cruz CD, Finley LWS, et al.
467 Adrenergic nerves activate an angio-metabolic switch in prostate cancer. Science.
468 2017;358(6361):321-6. doi: 10.1126/science.aah5072. PubMed PMID: 29051371; PubMed
469 Central PMCID: PMCPMC5783182.
470 15. Pirzgalska RM, Seixas E, Seidman JS, Link VM, Sanchez NM, Mahu I, et al. Sympathetic
471 neuron-associated macrophages contribute to obesity by importing and metabolizing
472 norepinephrine. Nat Med. 2017;23(11):1309-18. Epub 20171009. doi: 10.1038/nm.4422.
473 PubMed PMID: 29035364; PubMed Central PMCID: PMCPMC7104364.
474 16. Maryanovich M, Zahalka AH, Pierce H, Pinho S, Nakahara F, Asada N, et al. Adrenergic
475 nerve degeneration in bone marrow drives aging of the hematopoietic stem cell niche. Nat
476 Med. 2018;24(6):782-91. Epub 20180507. doi: 10.1038/s41591-018-0030-x. PubMed PMID:
477 29736022; PubMed Central PMCID: PMCPMC6095812.
478 17. Ishikawa G, Peng X, McGovern J, Woo S, Perry C, Liu A, et al. alpha1 Adrenoreceptor
479 antagonism mitigates extracellular mitochondrial DNA accumulation in lung fibrosis models and
480 in patients with idiopathic pulmonary fibrosis. Am J Physiol Lung Cell Mol Physiol.
481 2023;324(5):L639-L51. Epub 20230117. doi: 10.1152/ajplung.00119.2022. PubMed PMID:
482 36648147; PubMed Central PMCID: PMCPMC10110730.
483 18. Briest W, Homagk L, Rassler B, Ziegelhoffer-Mihalovicova B, Meier H, Tannapfel A, et al.
484 Norepinephrine-induced changes in cardiac transforming growth factor-beta isoform
485 expression pattern of female and male rats. Hypertension. 2004;44(4):410-8. Epub 20040823.
486 doi: 10.1161/01.HYP.0000141414.87026.4d. PubMed PMID: 15326086.
487 19. Gao R, Peng X, Perry C, Sun H, Ntokou A, Ryu C, et al. Macrophage-derived netrin-1
488 drives adrenergic nerve-associated lung fibrosis. J Clin Invest. 2021;131(1). doi:
489 10.1172/JCI136542. PubMed PMID: 33393489; PubMed Central PMCID: PMCPMC7773383.
490 20. Miki K, Maekura R, Hiraga T, Hashimoto H, Kitada S, Miki M, et al. Acidosis and raised
491 norepinephrine levels are associated with exercise dyspnoea in idiopathic pulmonary fibrosis.
492 Respirology. 2009;14(7):1020-6. doi: 10.1111/j.1440-1843.2009.01607.x. PubMed PMID:
493 19740262.
494 21. Gillis CN, Huxtable RJ, Roth RA. Effects of monocrotaline pretreatment of rats on
495 removal of 5-hydroxytryptamine and noradrenaline by perfused lung. Br J Pharmacol.
496 1978;63(3):435-43. doi: 10.1111/j.1476-5381.1978.tb07795.x. PubMed PMID: 667487; PubMed
497 Central PMCID: PMCPMC1668101.
498 22. Oriowo MA, Chandrasekhar B, Kadavil EA. Alpha 1-adrenoceptor subtypes mediating
499 noradrenaline-induced contraction of pulmonary artery from pulmonary hypertensive rats. Eur
500 J Pharmacol. 2003;482(1-3):255-63. doi: 10.1016/j.ejphar.2003.10.001. PubMed PMID:
501 14660030.

502 23. Reinhardt D. Adrenoceptors and the lung: their role in health and disease. Eur J Pediatr.
503 1989;148(4):286-93. doi: 10.1007/BF00444116. PubMed PMID: 2651128.
504 24. Salvi SS. Alpha1-adrenergic hypothesis for pulmonary hypertension. Chest.
505 1999;115(6):1708-19. doi: 10.1378/chest.115.6.1708. PubMed PMID: 10378571.
506 25. Neumark N, Cosme C, Jr., Rose KA, Kaminski N. The Idiopathic Pulmonary Fibrosis Cell
507 Atlas. Am J Physiol Lung Cell Mol Physiol. 2020;319(6):L887-L93. Epub 20200930. doi:
508 10.1152/ajplung.00451.2020. PubMed PMID: 32996785; PubMed Central PMCID:
509 PMCPMC7792683.
510 26. Rassler B, Marx G, Schierle K, Zimmer HG. Catecholamines can induce pulmonary
511 remodeling in rats. Cell Physiol Biochem. 2012;30(5):1134-47. Epub 20121005. doi:
512 10.1159/000343304. PubMed PMID: 23171784.
513 27. Rassler B. Role of alpha- and beta-adrenergic mechanisms in the pathogenesis of
514 pulmonary injuries characterized by edema, inflammation and fibrosis. Cardiovasc Hematol
515 Disord Drug Targets. 2013;13(3):197-207. doi: 10.2174/1871529x1303140129154602. PubMed
516 PMID: 24479719.
517 28. Dincer HE, Gangopadhyay N, Wang R, Uhal BD. Norepinephrine induces alveolar
518 epithelial apoptosis mediated by alpha-, beta-, and angiotensin receptor activation. Am J
519 Physiol Lung Cell Mol Physiol. 2001;281(3):L624-30. doi: 10.1152/ajplung.2001.281.3.L624.
520 PubMed PMID: 11504689.
521 29. Abraham E, Kaneko DJ, Shenkar R. Effects of endogenous and exogenous
522 catecholamines on LPS-induced neutrophil trafficking and activation. Am J Physiol.
523 1999;276(1):L1-8. doi: 10.1152/ajplung.1999.276.1.L1. PubMed PMID: 9887049.
524 30. Staedtke V, Bai RY, Kim K, Darvas M, Davila ML, Riggins GJ, et al. Disruption of a self-
525 amplifying catecholamine loop reduces cytokine release syndrome. Nature.
526 2018;564(7735):273-7. Epub 20181212. doi: 10.1038/s41586-018-0774-y. PubMed PMID:
527 30542164; PubMed Central PMCID: PMCPMC6512810.
528 31. Lu M, Fan X, Liao W, Li Y, Ma L, Yuan M, et al. Identification of significant genes as
529 prognostic markers and potential tumor suppressors in lung adenocarcinoma via
530 bioinformatical analysis. BMC Cancer. 2021;21(1):616. Epub 20210526. doi: 10.1186/s12885-
531 021-08308-3. PubMed PMID: 34039311; PubMed Central PMCID: PMCPMC8157630.
532 32. Muhl L, Mocci G, Pietila R, Liu J, He L, Genove G, et al. A single-cell transcriptomic
533 inventory of murine smooth muscle cells. Dev Cell. 2022;57(20):2426-43 e6. doi:
534 10.1016/j.devcel.2022.09.015. PubMed PMID: 36283392.
535 33. Kircali MF, Turanli B. Idiopathic Pulmonary Fibrosis Molecular Substrates Revealed by
536 Competing Endogenous RNA Regulatory Networks. OMICS. 2023;27(8):381-92. Epub 20230804.
537 doi: 10.1089/omi.2023.0072. PubMed PMID: 37540140.
538 34. Zhou Y, Peng H, Sun H, Peng X, Tang C, Gan Y, et al. Chitinase 3-like 1 suppresses injury
539 and promotes fibroproliferative responses in Mammalian lung fibrosis. Sci Transl Med.
540 2014;6(240):240ra76. doi: 10.1126/scitranslmed.3007096. PubMed PMID: 24920662; PubMed
541 Central PMCID: PMCPMC4340473.
542 35. Lee CG, Cho SJ, Kang MJ, Chapoval SP, Lee PJ, Noble PW, et al. Early growth response
543 gene 1-mediated apoptosis is essential for transforming growth factor beta1-induced
544 pulmonary fibrosis. J Exp Med. 2004;200(3):377-89. doi: 10.1084/jem.20040104. PubMed
545 PMID: 15289506; PubMed Central PMCID: PMCPMC2211975.

546 36. Mehdizadeh S, Taherian M, Bayati P, Mousavizadeh K, Pashangzadeh S, Anisian A, et al.
547 Plumbagin attenuates Bleomycin-induced lung fibrosis in mice. Allergy Asthma Clin Immunol.
548 2022;18(1):93. Epub 20221021. doi: 10.1186/s13223-022-00734-7. PubMed PMID: 36271442;
549 PubMed Central PMCID: PMCPMC9585773.
550 37. Depledge MH. Respiration and lung function in the mouse, Mus musculus (with a note
551 on mass exponents and respiratory variables). Respir Physiol. 1985;60(1):83-94. doi:
552 10.1016/0034-5687(85)90041-6. PubMed PMID: 4001609.
553 38. Schroeder WG, Mitrescu LM, Hart ML, Unnithan R, Gilchrist JM, Smith EE, et al. Flexible
554 low-cost system for small animal aerosol inhalation exposure to drugs, proteins, inflammatory
555 agents, and infectious agents. Biotechniques. 2009;46(3 Suppl):Piii-Pviii. doi:
556 10.2144/000112895. PubMed PMID: 19317668.
557 39. McGovern TK, Robichaud A, Fereydoonzad L, Schuessler TF, Martin JG. Evaluation of
558 respiratory system mechanics in mice using the forced oscillation technique. J Vis Exp.
559 2013;(75):e50172. Epub 20130515. doi: 10.3791/50172. PubMed PMID: 23711876; PubMed
560 Central PMCID: PMCPMC3684007.
561 40. Hubner RH, Gitter W, El Mokhtari NE, Mathiak M, Both M, Bolte H, et al. Standardized
562 quantification of pulmonary fibrosis in histological samples. Biotechniques. 2008;44(4):507-11,
563 14-7. doi: 10.2144/000112729. PubMed PMID: 18476815.
564 41. Urushiyama H, Terasaki Y, Nagasaka S, Kokuho N, Endo Y, Terasaki M, et al. Naftopidil
565 reduced the proliferation of lung fibroblasts and bleomycin-induced lung fibrosis in mice. J Cell
566 Mol Med. 2019;23(5):3563-71. Epub 20190315. doi: 10.1111/jcmm.14255. PubMed PMID:
567 30873733; PubMed Central PMCID: PMCPMC6484423.
568 42. Serna-Salas SA, Arroyave-Ospina JC, Zhang M, Damba T, Buist-Homan M, Munoz-Ortega
569 MH, et al. alpha-1 Adrenergic receptor antagonist doxazosin reverses hepatic stellate cells
570 activation via induction of senescence. Mech Ageing Dev. 2022;201:111617. Epub 20211224.
571 doi: 10.1016/j.mad.2021.111617. PubMed PMID: 34958827.
572 43. Perlini S, Palladini G, Ferrero I, Tozzi R, Fallarini S, Facoetti A, et al. Sympathectomy or
573 doxazosin, but not propranolol, blunt myocardial interstitial fibrosis in pressure-overload
574 hypertrophy. Hypertension. 2005;46(5):1213-8. Epub 20051010. doi:
575 10.1161/01.HYP.0000185689.65045.4c. PubMed PMID: 16216989.
576 44. Pawluczyk IZ, Patel SR, Harris KP. The role of the alpha-1 adrenoceptor in modulating
577 human mesangial cell matrix production. Nephrol Dial Transplant. 2006;21(9):2417-24. Epub
578 20060516. doi: 10.1093/ndt/gfl230. PubMed PMID: 16705025.
579 45. Koenecke A, Powell M, Xiong R, Shen Z, Fischer N, Huq S, et al. Alpha-1 adrenergic
580 receptor antagonists to prevent hyperinflammation and death from lower respiratory tract
581 infection. Elife. 2021;10. Epub 20210611. doi: 10.7554/eLife.61700. PubMed PMID: 34114951;
582 PubMed Central PMCID: PMCPMC8195605.
583 46. Li S, Jun T, Tyler J, Schadt E, Kao YH, Wang Z, et al. Inpatient Administration of Alpha-1-
584 Adrenergic Receptor Blocking Agents Reduces Mortality in Male COVID-19 Patients. Front Med
585 (Lausanne). 2022;9:849222. Epub 20220228. doi: 10.3389/fmed.2022.849222. PubMed PMID:
586 35295598; PubMed Central PMCID: PMCPMC8919772.
587 47. Munoz-Ortega MH, Llamas-Ramirez RW, Romero-Delgadillo NI, Elias-Flores TG, Tavares-
588 Rodriguez Ede J, Campos-Esparza Mdel R, et al. Doxazosin Treatment Attenuates Carbon
589 Tetrachloride-Induced Liver Fibrosis in Hamsters through a Decrease in Transforming Growth

590 Factor beta Secretion. Gut Liver. 2016;10(1):101-8. doi: 10.5009/gnl14459. PubMed PMID:
591 26573293; PubMed Central PMCID: PMCPMC4694741.
592 48. Barnes PJ, Wilson NM, Vickers H. Prazosin, an alpha 1-adrenoceptor antagonist, partially
593 inhibits exercise-induced asthma. J Allergy Clin Immunol. 1981;68(6):411-5. doi: 10.1016/0091-
594 6749(81)90193-7. PubMed PMID: 6118384.
595 49. Koshimizu TA, Tanoue A, Hirasawa A, Yamauchi J, Tsujimoto G. Recent advances in
596 alpha1-adrenoceptor pharmacology. Pharmacol Ther. 2003;98(2):235-44. doi: 10.1016/s0163-
597 7258(03)00033-0. PubMed PMID: 12725871.
598 50. Kyncl JJ. Pharmacology of terazosin. Am J Med. 1986;80(5B):12-9. doi: 10.1016/0002-
599 9343(86)90846-6. PubMed PMID: 2872801.
600 51. Li H, Xu TY, Li Y, Chia YC, Buranakitjaroen P, Cheng HM, et al. Role of alpha1-blockers in
601 the current management of hypertension. J Clin Hypertens (Greenwich). 2022;24(9):1180-6.
602 doi: 10.1111/jch.14556. PubMed PMID: 36196467; PubMed Central PMCID: PMCPMC9532918.
603 52. Butt AK, Patel J, Shirwany H, Mirza Q, Hoover J, Khouzam RN. Beneficial Extracardiac
604 Effects of Cardiovascular Medications. Curr Cardiol Rev. 2022;18(2):e151021197270. doi:
605 10.2174/1573403X17666211015145132. PubMed PMID: 34779371; PubMed Central PMCID:
606 PMCPMC9413730.
607 53. Somberg JC, Achari R, Laddu AR. Terazosin: pharmacokinetics and the effect of age and
608 dose on the incidence of adverse events. Am Heart J. 1991;122(3 Pt 2):901-5. doi:
609 10.1016/0002-8703(91)90809-v. PubMed PMID: 1678920.
610 54. Goldie RG, Lulich KM, Paterson JW. Bronchial Alpha-Adrenoceptor Function in Asthma.
611 Trends Pharmacol Sci. 1985;6(12):469-72. doi: Doi 10.1016/0165-6147(85)90225-1. PubMed
612 PMID: WOS:A1985AXH3500012.
613 55. Barnes PJ, Ind PW, Dollery CT. Inhaled prazosin in asthma. Thorax. 1981;36(5):378-81.
614 doi: 10.1136/thx.36.5.378. PubMed PMID: 6118964; PubMed Central PMCID: PMCPMC471513.
615 56. Black JL, Salome C, Yan K, Shaw J. The action of prazosin and propylene glycol on
616 methoxamine-induced bronchoconstriction in asthmatic subjects. Br J Clin Pharmacol.
617 1984;18(3):349-53. doi: 10.1111/j.1365-2125.1984.tb02475.x. PubMed PMID: 6487474;
618 PubMed Central PMCID: PMCPMC1463636.
619 57. Strickland NH, Hughes JM, Hart DA, Myers MJ, Lavender JP. Cause of regional
620 ventilation-perfusion mismatching in patients with idiopathic pulmonary fibrosis: a combined
621 CT and scintigraphic study. AJR Am J Roentgenol. 1993;161(4):719-25. doi:
622 10.2214/ajr.161.4.8372745. PubMed PMID: 8372745.
623 58. Usmani OS, Biddiscombe MF, Yang S, Meah S, Oballa E, Simpson JK, et al. The topical
624 study of inhaled drug (salbutamol) delivery in idiopathic pulmonary fibrosis. Respir Res.
625 2018;19(1):25. Epub 20180206. doi: 10.1186/s12931-018-0732-0. PubMed PMID: 29409488;
626 PubMed Central PMCID: PMCPMC5801831.
627 59. Bai X, Zhao G, Chen Q, Li Z, Gao M, Ho W, et al. Inhaled siRNA nanoparticles targeting
628 IL11 inhibit lung fibrosis and improve pulmonary function post-bleomycin challenge. Sci Adv.
629 2022;8(25):eabn7162. Epub 20220622. doi: 10.1126/sciadv.abn7162. PubMed PMID:
630 35731866; PubMed Central PMCID: PMCPMC9216512.
631

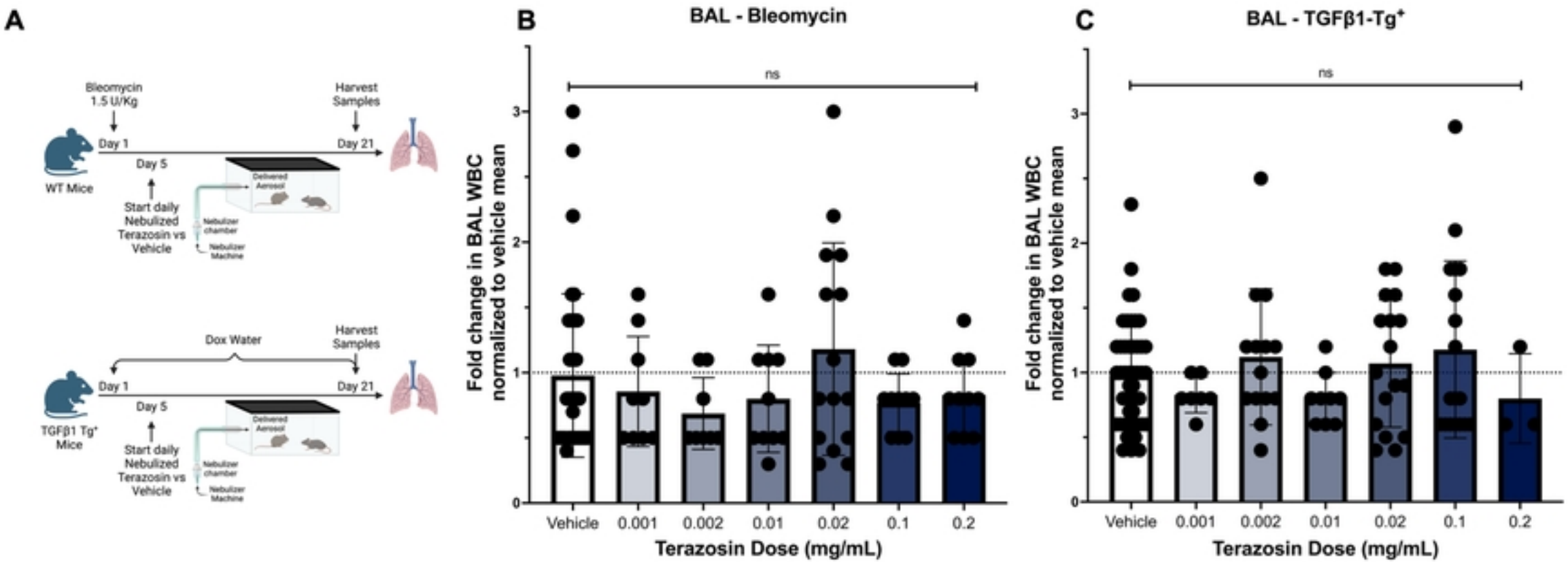
A
Bleomycin
1.5 U/Kg
Harvest
Samples
Day 1
Day 21
Day 5
WT Mice
Start daily
Nebulized
Terazosin vs
Vehicle
Dox Water
Harvest
Samples
Day 1
Day 21
Day 5
TGFβ1 Tg+
Mice
Start daily
Nebulized
Terazosin vs
Vehicle
B
BAL - Bleomycin
ns
Fold change in BAL WBC
normalized to vehicle mean
Vehicle
0.001
0.002
0.01
0.02
0.1
0.2
Terazosin Dose (mg/mL)
C
BAL - TGFβ1-Tg+
ns
Fold change in BAL WBC
normalized to vehicle mean
Vehicle
0.001
0.002
0.01
0.02
0.1
0.2
Terazosin Dose (mg/mL)

Figure 1

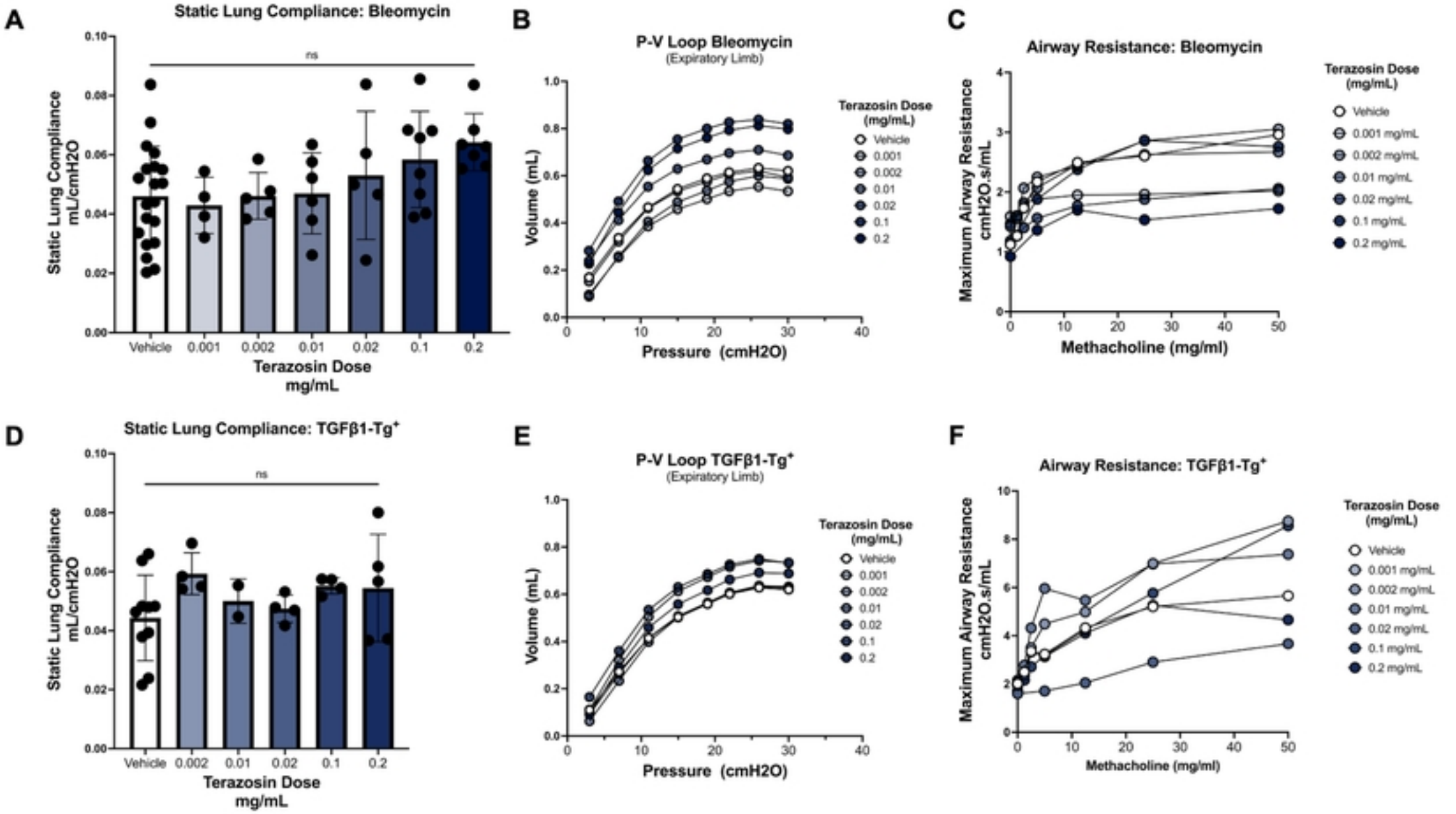
A
Static Lung Compliance: Bleomycin
ns
Static Lung Compliance mL/cmH2O
Vehicle
0.001
0.002
0.01
0.02
0.1
0.2
Terazosin Dose mg/mL
B
P-V Loop Bleomycin
(Expiratory Limb)
Volume (mL)
Pressure (cmH2O)
Terazosin Dose (mg/mL)
C
Airway Resistance: Bleomycin
Maximum Airway Resistance cmH2O.s/mL
Methacholine (mg/ml)
Terazosin Dose (mg/mL)
0.001 mg/mL
0.002 mg/mL
0.01 mg/mL
0.02 mg/mL
0.1 mg/mL
0.2 mg/mL
D
Static Lung Compliance: TGFβ1-Tg+
E
P-V Loop TGFβ1-Tg+
(Expiratory Limb)
F
Airway Resistance: TGFβ1-Tg+

Figure 2

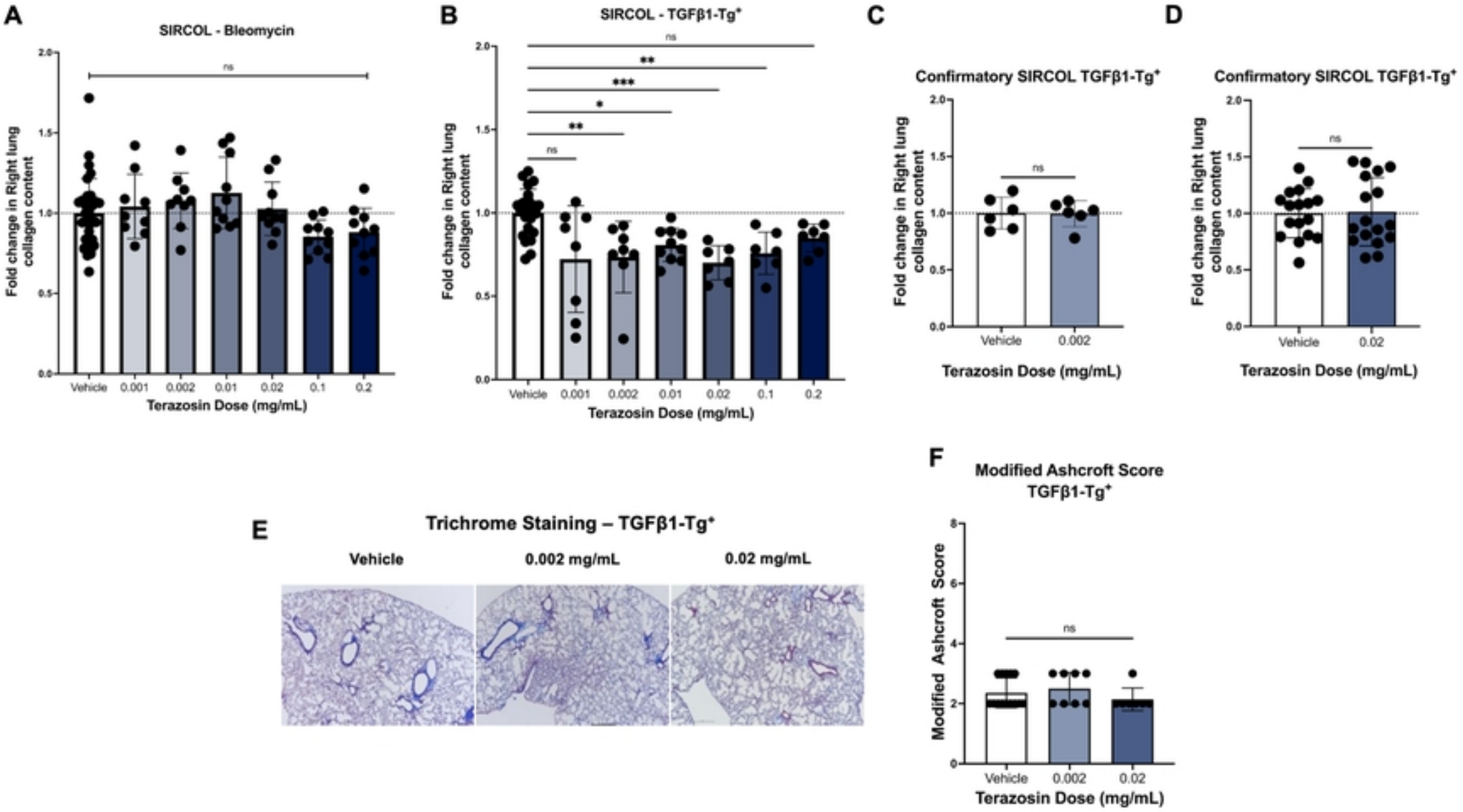
A
SIRCOL - Bleomycin
ns
Fold change in Right lung collagen content
Vehicle
0.001
0.002
0.01
0.02
0.1
0.2
Terazosin Dose (mg/mL)
B
SIRCOL - TGFβ1-Tg+
ns
**
***
*
**
ns
Fold change in Right lung collagen content
Vehicle
0.001
0.002
0.01
0.02
0.1
0.2
Terazosin Dose (mg/mL)
C
Confirmatory SIRCOL TGFβ1-Tg+
ns
Fold change in Right lung collagen content
Vehicle
0.002
Terazosin Dose (mg/mL)
D
Confirmatory SIRCOL TGFβ1-Tg+
ns
Fold change in Right lung collagen content
Vehicle
0.02
Terazosin Dose (mg/mL)
E
Trichrome Staining – TGFβ1-Tg+
Vehicle
0.002 mg/mL
0.02 mg/mL
F
Modified Ashcroft Score
TGFβ1-Tg+
ns
Modified Ashcroft Score
Vehicle
0.002
0.02
Terazosin Dose (mg/mL)

Figure 3

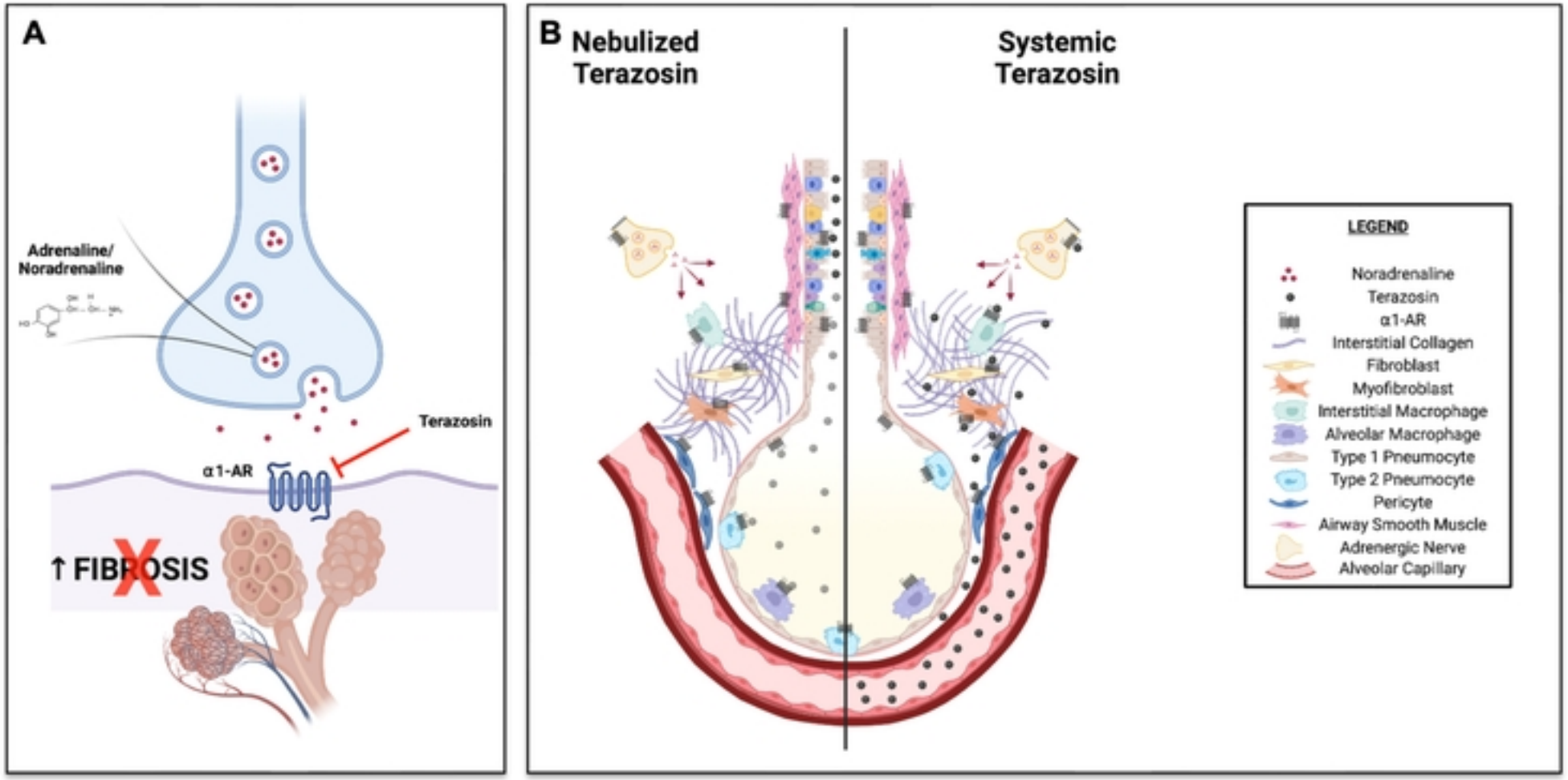
A
Adrenaline/
Noradrenaline
Terazosin
α1-AR
↑ FIBROSIS
B
Nebulized
Terazosin
Systemic
Terazosin
LEGEND
Noradrenaline
Terazosin
α1-AR
Interstitial Collagen
Fibroblast
Myofibroblast
Interstitial Macrophage
Alveolar Macrophage
Type 1 Pneumocyte
Type 2 Pneumocyte
Pericyte
Airway Smooth Muscle
Adrenergic Nerve
Alveolar Capillary

Figure 4